

## Slip at liquid-liquid interfaces

P. Poesio and A. Damone

*Department of Mechanical and Industrial Engineering, Università degli Studi di Brescia,  
Via Branze 38, 25123 Brescia, Italy*

Omar K. Matar

*Department of Chemical Engineering, Imperial College London, South Kensington Campus,  
London SW7 2AZ, United Kingdom*

(Received 30 August 2016; published 27 April 2017)

We address a problem of fundamental importance in the physics of interfaces, which is central to the description of multiphase fluid dynamics. This work is important to study interfaces in systems such as polymer melts and solutions, where velocity jumps have been observed and interpreted as a manifestation of slip. This is in violation of classical interfacial conditions that require continuity of velocity and has been remedied in the literature via use of *ad hoc* models, such as the so-called Navier slip condition. This paper suggests that it is possible to obviate completely the need for such an approach. Instead, we show that one simply requires knowledge of the density field and the molar fraction of the fluid components and the dependence of the viscosity on the density. This information can be obtained easily through molecular dynamics simulations.

DOI: [10.1103/PhysRevFluids.2.044004](https://doi.org/10.1103/PhysRevFluids.2.044004)

### I. INTRODUCTION

The classical boundary conditions at flat liquid-liquid interfaces are continuity of the velocity and of the tangential component of stress [1]; for curved interfaces, one also demands that the jump in the normal stress at the interface is balanced by the product of the interfacial tension and curvature. While these conditions are widely accepted and are often used at the macroscale, the recent interest in microfluidics [2,3] and nanofluidics [4] challenges their validity. At molten polymer-polymer interfaces, for instance, it has been consistently shown by direct and indirect measurements [5,6] that, apparent velocity jumps exist and can be modeled effectively via a Navier slip condition (NSC). Here we discuss that if a viscosity, which accounts for the density and mole fraction distributions, is included in the Navier-Stokes equations, we can describe, naturally and without recourse to *ad hoc* models such as the NSC, the velocity profile in the interfacial region separating two fluids. This approach is supported by the observation that there is a relation between the apparent slip and density distribution across the interface [7].

To implement our idea, we simply need to know the density distribution  $\rho$  and the molar fraction  $\chi$  [which can be obtained, for instance, via molecular dynamics (MD) simulations [8–12], a diffuse interface approach [13,14], or density functional theory (DFT) [15]] everywhere within the fluids, even at the interface, where regions of rapid density variations may occur due to molecular interactions. We also need a constitutive relation such as  $\mu = \mu(\rho, \chi)$ , which can be obtained by MD or any other theoretical means [16]. Since all that we need are fluid (or mixture) properties, no other interfacial conditions are required to describe the apparent slip [7,17], which can be found by classical continuum theory.

The apparent slip velocity at polymer-polymer interfaces (normally related to chain conformation and entanglement) has been well studied and reported experimentally by several investigators [5,6]; for simple fluids, only a few recent MD simulations pinpoint the presence of an apparent slip velocity, i.e., a region whose thickness is of the molecular size, close to the interface where the velocity changes very rapidly. Similarly to solid-liquid interfaces [18], this rapid change is replaced by a velocity jump  $\Delta u$  and described by a NSC [7,19]  $\Delta u = \alpha \tau$ , where  $\Delta u$  is proportional to the shear stress  $\tau$

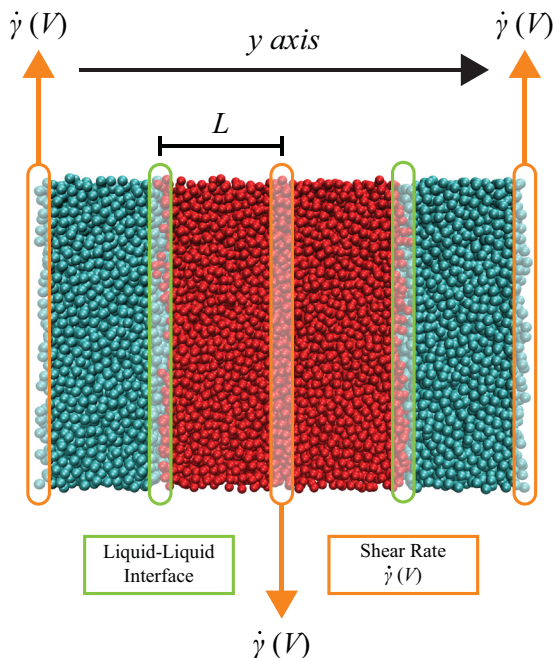


FIG. 1. Setup used to initialize the MD simulations.

through a slip length  $\alpha$ . Another possibility is the introduction of an interfacial viscosity [17] within a layer (whose thickness must be determined by previous MD simulations) across the interface. While both strategies prove effective in describing the velocity profile far from the interface, they require case-specific information: A MD simulation must be carried out to extract, for instance, the slip length, which is then used as an interfacial condition for the solution of the Navier-Stokes equations. These approaches lack generality and cannot describe the very rapid velocity transition across the interface, which is simply replaced by an unphysical discontinuity in the velocity profile. Different mixtures are used to show that if the effect of density and mole fraction variations on the viscosity are accounted for, then the Navier-Stokes equations can predict the full velocity profile, including, crucially, the rapid change in velocity across the interface, which is often interpreted as apparent slip. In this work we show that taking different properties (which can be independently measured, such as density distribution or viscosity), we can properly predict the velocity distribution across the interface. This approach implies and demonstrates that the velocity distribution is not affected by any additional properties, such as the slip length, but it is encapsulated in the actual fluid properties.

## II. SIMULATION DETAILS

As a test geometry, let us consider a steady Couette flow [1] between two planes at  $y = \pm L$  with the streamwise component of the velocity  $u(y = \pm L) = \pm V$ , of two liquids, with the interface at  $y = 0$ ; here  $y$  represents the wall-normal direction and  $L$  and  $V$  are constants as shown by the setup depicted in Fig. 1. Accounting for  $\rho$  and  $\chi$  variations (and hence viscosity changes) across the interface, the Navier-Stokes equations simplify to

$$\frac{d}{dy} \left[ \mu(\rho, \chi) \left( \frac{du}{dy} \right) \right] = 0. \quad (1)$$

To solve this equation, we need to provide the constitutive relation for the viscosity  $\mu = \mu(\rho, \chi)$  and the density and mole fraction distributions across the interface  $\rho = \rho(y)$ . All cases described here are

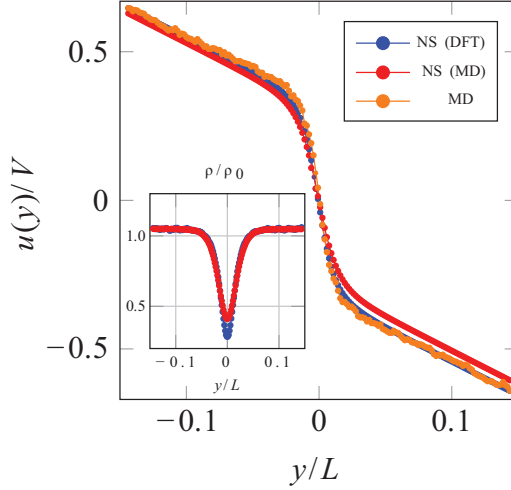


FIG. 2. Close-up of the normalized streamwise velocity component in the interfacial region, obtained via MD simulations (orange line), and solution of the Navier-Stokes equations with  $\mu(\rho)$  calculated using DFT (blue line) and MD (red line) for the case of two immiscible, symmetrical Lennard-Jones fluids ( $V = 25$  m/s,  $L = 46.65$  Å, and  $L_x = L_z = 108.34$  Å). The density (see the inset, where  $\rho_0 = 1.1705$  g/ml) used to solve the NS equations was obtained from DFT (blue line) and MD simulations (red line). The MD simulation uses 17 248 particles for each fluid.

in the creeping flow limit, with Reynolds number  $Re = \rho V L / \mu \ll 1$  and a Deborah number [based on the shear rate  $\dot{\gamma}$  and on the molecular time scale  $t = m^{1/2} \sigma / \epsilon^{1/2}$ , where  $m$  is the molecular mass and  $\sigma$  and  $\epsilon$  are the interaction parameters; see Eq. (2)] on the order of  $De = \dot{\gamma} t \sim 10^{-2}$ , for which only Newtonian behavior is expected. Deviation from non-Newtonian behavior, such as Carreau fluid, can be accounted for provided a constitutive relation, which depends upon  $\dot{\gamma}$ , is provided; in that case,  $\mu = \mu(\rho, \chi, \dot{\gamma})$ .

### III. RESULTS

#### A. Atomic fluids

All simulations are carried out with an *NVT* ensemble and thermostated by a Nosé-Hoover thermostat at  $T = 130$  K. The first example is given by two identical immiscible atomic fluids. The interaction between the particles of two liquids is given by a modified Lennard-Jones potential

$$U_{ij} = 4\epsilon \left[ \left( \frac{\sigma}{r_{ij}} \right)^6 - \beta_{ij} \left( \frac{\sigma}{r_{ij}} \right)^{12} \right]. \quad (2)$$

The  $\beta_{ij}$  parameter allows variation of the miscibility between the two fluids  $i$  and  $j$ . Here  $\beta_{ij} = 1$  if  $i = j$ ; if  $i \neq j$ , the parameter  $\beta_{ij}$  is used to change the miscibility of the two liquids:  $0 \leq \beta_{ij} \leq 1$  corresponds to partial miscibility, with complete immiscibility and miscibility being represented by  $\beta_{ij} = 0$  and  $\beta_{ij} = 1$ , respectively. The values of  $\epsilon$  and  $\sigma$  are  $\epsilon/k_B = 120$  K and  $\sigma = 3.4$  Å with a cutoff radius  $r_c = 3.1 \sigma$  and  $k_B$  is the Boltzmann constant. The mass  $M$  is taken equal to  $M = 39.948$  g/mol. This simplified case allows us to compute the density and mole fraction profiles across the interface using DFT [15] (see Fig. 2); the viscosity distribution is then computed using a theoretical approach developed for a strongly inhomogeneous Lennard-Jones fluid [16]. Substitution of the relation  $\mu(\rho, \chi)$  into the Navier-Stokes equations and their subsequent numerical solution yields the results shown in Fig. 2. As can be seen, the agreement with the predictions of the full MD simulations is very good.

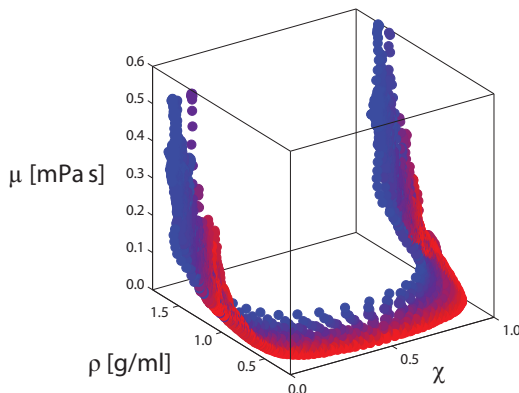


FIG. 3. Constitutive relations  $\mu = \mu(\rho, \chi)$  for two Lennard-Jones fluids with  $\beta_{ij} = 0$  at the same mass  $M$ , using 1400 particles for each liquid starting from  $L = 24.752 \text{ \AA}$  (blue circles) to  $L = 29.274 \text{ \AA}$  (red circles), and  $L_x = L_z = 35.36 \text{ \AA}$ .

The viscosity distribution  $\mu(\rho(y), \chi(y))$  is obtained using the distribution of  $\rho(y)$  and  $\chi(y)$  at equilibrium conditions and therefore does not depend upon the specific state. This is in contrast with the other approaches where the nonequilibrium properties, such as slip length [18] and interfacial viscosity [17], depend upon the specific state, characterized, for instance, by the imposed shear rate  $\dot{\gamma}$ . As the fluid structure and the intermolecular interactions become more complex, however, the required information cannot be obtained via a purely theoretical approach and MD becomes the only feasible option. If we extract from the MD simulations the relation  $\mu(\rho(y), \chi(y))$  for the case we have just described, we can see from Fig. 2 that the results compare very well in this case as well; here the constitutive relation  $\mu(\rho(y), \chi(y))$  is computed through equilibrium MD simulations, taking advantage of the well-known Muller-Plathe (nonequilibrium) method as shown in Fig. 3. The constitutive relation here is characteristic for this type of fluid, while other fluid will be characterized by other relations. The density distribution across the interface is computed by equilibrium simulation, namely, without any shear velocity imposed at the boundary.

In Fig. 4 we show the same results for two (symmetrical) Lennard-Jones fluids with different levels of miscibility, induced by changing the interaction parameter  $\beta$ . Changing the interaction (between the two fluids) results in different density profiles at the interface; when we move from complete immiscibility ( $\beta = 0$ ) to full miscibility ( $\beta = 1$ ), the density profile changes and the dip (molecular depletion region) gradually reduces to zero at full miscibility. The dip occurs because the energetically unfavorable interactions between the two fluids are concentrated at the interface. The system can lower its free energy by decreasing the overall density at the interface as this reduces the number of particle interactions. The size of the dip is determined by balancing this energy gain against the entropic cost of denying particles at the interface some volume. Due to molecular depletion, the shear viscosity at the interfaces is lower than in the bulk region, showing that the transport of momentum in the former region is less efficient than in the bulk; to balance the viscosity decrease, the velocity gradient increases, as shown in Fig. 4, leading to apparent slip. As the density contrast decreases, the associated variation in the velocity profile becomes less steep and the apparent slip reduces. If we introduce the corresponding density variation into the Navier-Stokes equations, numerical solutions of the latter are in excellent agreement with MD predictions.

In Fig. 5 we show that our approach is valid for different imposed shear rate  $\dot{\gamma}$ , without requiring new or *ad hoc* conditions, as opposed to approaches that rely on the use of slip models [7,18]. The density distribution does not depend on  $\dot{\gamma}$ , supporting the choice of computing at equilibrium conditions. In Fig. 6 we compare the results for two Lennard-Jones fluids with

## SLIP AT LIQUID-LIQUID INTERFACES

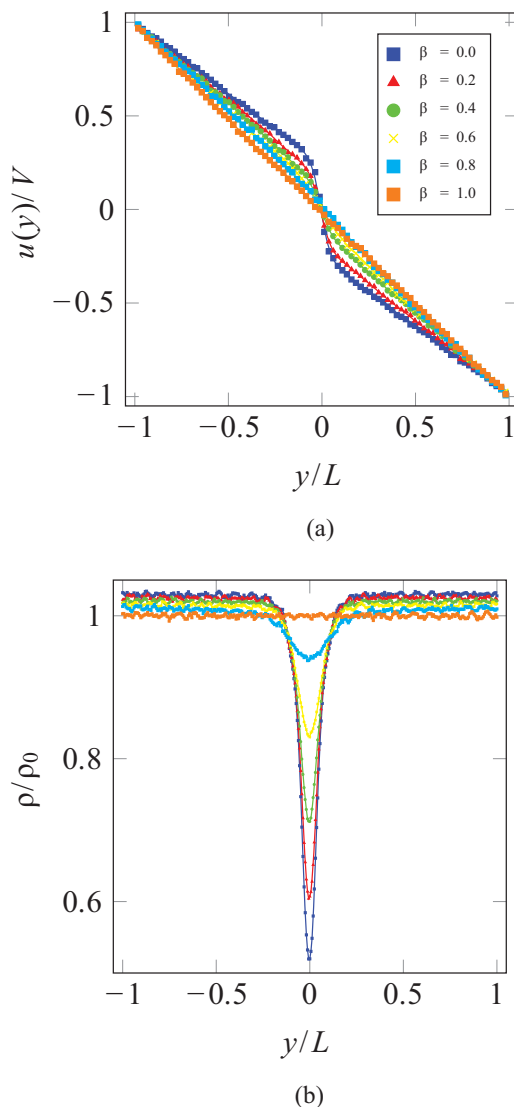


FIG. 4. Normalized streamwise velocity component ( $V = 50$  m/s,  $L = 40.205$  Å, and  $L_x = L_z = 108.34$  Å) across the interface (a) obtained for different density distributions [ $\rho(\gamma = 0) \equiv \rho_0 = 1.36$  g/ml] and (b) calculated by varying the parameter  $\beta_{ij}$  in the intermolecular potential (2) used in the MD simulations. The Navier-Stokes solutions that use these distributions and MD velocity predictions are shown in (a) by the solid lines and symbols, respectively. The MD simulations use 17 248 particles for each fluid.

different molecular masses by varying the mass of one fluid to 3 and 5 times the mass of the first fluid ( $M = 39\,948$  g/mol), which induces an asymmetry in the density. Once again, when the Navier-Stokes equations are solved with a density-dependent viscosity, the results compare extremely well with those obtained from MD.

### B. Real fluids

In Fig. 7 we present results for water–carbon tetrachloride, water–octane, and heptane–ethylene glycol systems. These fluids are very well documented using both MD and DFT theory and their

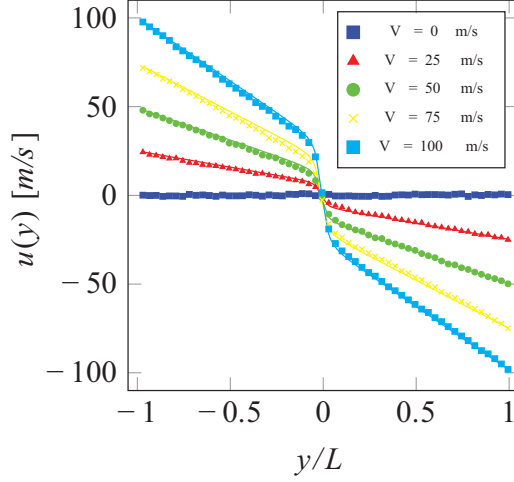


FIG. 5. Streamwise velocity component calculated from the Navier-Stokes equations (solid lines) and MD simulations (symbols), obtained for different shear rates ( $L = 40.205 \text{ \AA}$  and  $L_x = L_z = 108.34 \text{ \AA}$ )  $\dot{\gamma}$  with  $\beta_{ij} = 0$ . The MD simulations use 17 248 particles for each fluid.

simulations are carried out using standard models. In particular, for water, we used the TIP4P/2005 model [20]; for the other fluids, we used the optimized potential for liquid all-atom simulations (see Ref. [21]). Interatomic interaction parameters are obtained by the Lorentz-Berthelot mixing rules. All simulations are carried out with an  $NVT$  ensemble and thermostated by a Nosé-Hoover thermostat at  $T = 303.15 \text{ K}$ . The number of molecules is changed to obtain different density and mole fractions. Even for these complex cases, if we account for the dependence of the viscosity on the density profile across the interface, the Navier-Stokes equations predict the velocity distribution close to the interface and far away from it. When no molecular depletion is present at the

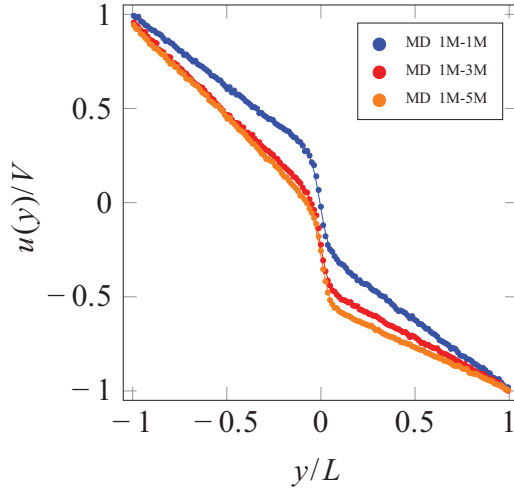


FIG. 6. Normalized streamwise velocity component ( $V = 50 \text{ m/s}$ ,  $L = 40.205 \text{ \AA}$ , and  $L_x = L_z = 108.34 \text{ \AA}$ ) obtained from the Navier-Stokes predictions (solid lines) and MD simulations (symbols) for different immiscible fluids  $\beta_{ij} = 0$  by varying the molecular mass  $M$ . The MD simulations use 17 248 particles for each fluid.

## SLIP AT LIQUID-LIQUID INTERFACES

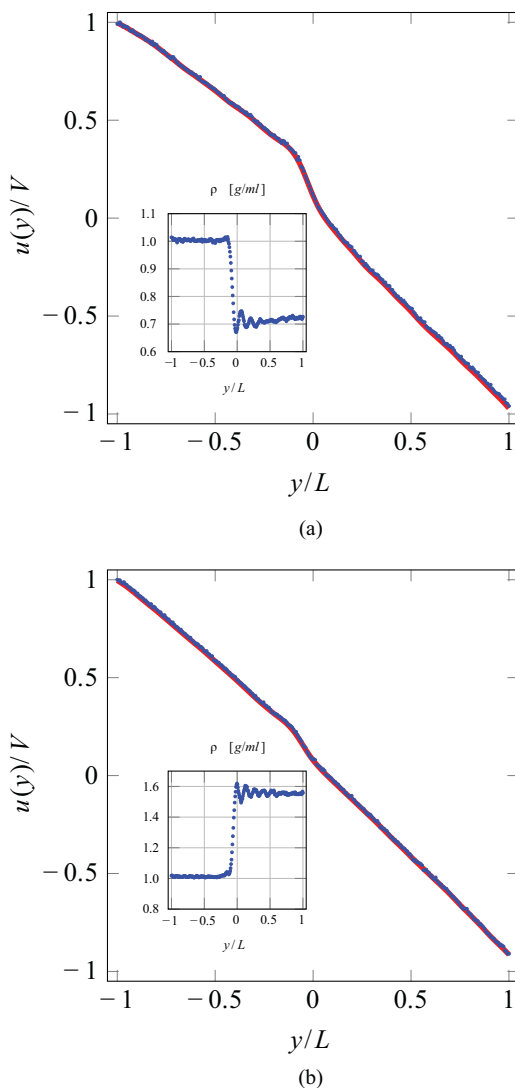


FIG. 7. Comparison between the normalized streamwise velocity profiles computed using MD simulations (symbols) and solutions of the Navier-Stokes equations (lines) for (a) the water-octane system ( $V = 100$  m/s,  $L = 29.46$  Å, and  $L_x = L_z = 35.01$  Å) and (b) the water-carbon tetrachloride system ( $V = 100$  m/s,  $L = 35.62$  Å, and  $L_x = L_z = 46.00$  Å). The insets show the variation of the density obtained using MD simulations.

(water-carbon tetrachloride) interface, the velocity profile is smooth and virtually no apparent slip occurs; on the other hand, when a density contrast develops due to molecular repulsion, apparent slip is clearly evident. The same conclusion holds for a simple Lennard-Jones mixture (see Fig. 4).

As a final test, we perform a similar comparison for the case of the heptane-ethylene glycol interface as shown in Fig. 8. For this system, we compute the density and the mole fraction distribution via DFT and we use them to compute the viscosity profile and thereafter the velocity profile. The comparison with the velocity profile obtained via the full MD simulation in this case is also excellent.

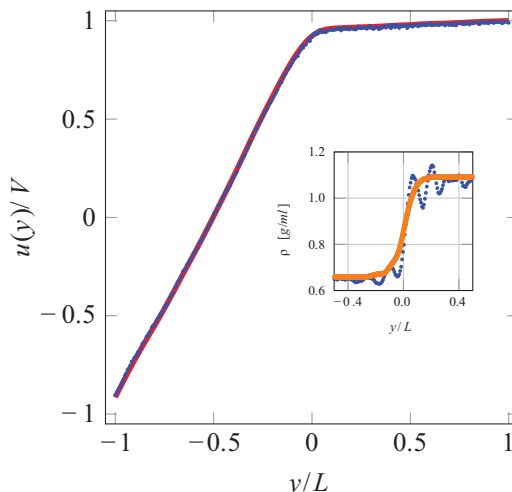


FIG. 8. Comparison between the normalized streamwise velocity profiles computed using MD simulations (symbols) and solutions of the Navier-Stokes equations (red line) for the heptane–ethylene glycol system ( $V = 100$  m/s,  $L = 30.31$  Å, and  $L_x = L_z = 34.93$  Å). The inset shows the variation of the density in the interfacial region obtained using MD simulations (symbols) and DFT (orange line).

#### IV. CONCLUSION

We have shown that the apparent slip velocity results from a molecular depletion at the interface, which is a direct consequence of the molecular interactions and therefore a property of the fluids not of shear rate  $\dot{\gamma}$ . When the two fluids are well mixed at the interface, no apparent slip is present. This conclusion is further supported by the observation that the density distribution, which in turn determines the apparent slip, does not depend on the shear rate (as long as the fluids behave in a Newtonian manner), but only on the intermolecular interactions. Furthermore, we have shown that if we account for the viscosity dependence on the density variation across the interface, the Navier-Stokes equations can be used to predict the velocity distribution throughout the domain, without the need for *ad hoc* boundary conditions such as slip models, but all the properties can be independently measured. There are no detailed measurements for the distribution of velocity at liquid-liquid interfaces.

#### ACKNOWLEDGMENTS

The authors acknowledge support from the Royal Society through their International Exchanges Scheme (Grant No. IE141486) and the Engineering and Physical Sciences Research Council, UK, through the MEMPHIS program (Grant No. EP/K003976/1). P.P. and A.D. acknowledge support from MIUR under the PRIN project.

- 
- [1] G. K. Batchelor, *An Introduction to Fluid Dynamics* (Cambridge University Press, Cambridge, 1967).  
 [2] J. Atencia and D. Beebe, Controlled microfluidic interfaces, *Nature (London)* **437**, 648 (2005).  
 [3] S. Pleasants, On-chip router, *Nat. Photon.* **8**, 85 (2014).  
 [4] W. Sparreboom, A. van der Berg, and J. C. T. Eijkel, Principles and applications of nanofluidic transport, *Nat. Nanotechnol.* **4**, 713 (2009).

- [5] R. Zhao and C. W. Macosko, Experimental determination of interfacial slip between polyethylene and thermoplastic elastomers, *J. Rheol.* **46**, 145 (2002).
- [6] P. C. Lee, H. E. Park, D. C. Morse, and C. W. Macosko, Polymer-polymer interfacial slip in multilayered films, *J. Rheol.* **53**, 893 (2009).
- [7] S. Razavi, J. Koplik, and I. Kretzschmar, Molecular dynamics simulations: Insight into molecular phenomena at interfaces, *Langmuir* **30**, 11272 (2014).
- [8] E. Diaz-Herrera, J. Alejandre, G. Ramirez-Santiago, and F. Forstmann, Interfacial tension behavior of binary and ternary mixtures of partially miscible Lennard-Jones fluids: A molecular dynamics simulation, *J. Chem. Phys.* **110**, 8084 (1999).
- [9] J. Stecki and S. Toxvaerd, Correlations in the liquid interfaces of simple liquids, *J. Chem. Phys.* **103**, 9763 (1995).
- [10] J. B. Buhn, P. A. Bopp, and M. J. Hampe, A molecular dynamics study of a liquid-liquid interface, *Fluid Phase Equilib.* **224**, 221 (2004).
- [11] H. A. Patel, E. B. Nauman, and S. Garde, Molecular structure and hydrophobic solvation thermodynamics at an octane-water interface, *J. Chem. Phys.* **119**, 9199 (2003).
- [12] S. Senapati and M. L. Berkowitz, Computer Simulation Study of the Interface Width of the Liquid/Liquid Interface, *Phys. Rev. Lett.* **87**, 176101 (2001).
- [13] L. M. Pismen, Nonlocal diffuse interface theory of thin films and the moving contact line, *Phys. Rev. E* **64**, 021603 (2001).
- [14] R. Mauri, *Non-Equilibrium Thermodynamics in Multiphase Flows* (Springer, Berlin, 2013).
- [15] I. Napari, A. Laaksonen, V. Talanquer, and D. W. Oxtoby, A density functional study of liquid-liquid interfaces in partially miscible systems, *J. Chem. Phys.* **110**, 5906 (1999).
- [16] H. Hoang and G. Galliero, Local shear viscosity of strongly inhomogeneous dense fluids: From the hard-sphere to the Lennard-Jones fluids, *J. Phys.: Condens. Matter* **25**, 485001 (2013).
- [17] G. Galliero, Lennard-Jones fluid-fluid interfaces under shear, *Phys. Rev. E* **81**, 056306 (2010).
- [18] P. A. Thompson and S. Troian, A general boundary condition for liquid flow at solid surfaces, *Nature (London)* **389**, 360 (1997).
- [19] Q. Ehlinger, L. Joly, and O. Pierre-Louis, Giant Slip at Liquid-Liquid Interfaces Using Hydrophobic Ball Bearings, *Phys. Rev. Lett.* **110**, 104504 (2013).
- [20] J. L. F. Abascal and C. Vega, A general purpose model for the condensed phases of water: TIP4P/2005, *J. Chem. Phys.* **123**, 234505 (2005).
- [21] W. L. Jorgensen, D. S. Maxwell, and J. Tirado-Rives, Development and testing of the OPLS all-atom force field on conformational energetics and properties of organic liquids, *J. Am. Soc. Chem.* **118**, 11225 (1996).